Preequilibrium neutron emission in heavy ion reaction: Mean field effect and multiple emission

Sabyasachi Paul,[1] Maitreyee Nandy,[2,*] A. K. Mohanty,[2] and Y. K. Gambhir[3,4]
[1]*Health Physics Division, Bhabha Atomic Research Centre, Mumbai 400085, India*
[2]*Saha Institute of Nuclear Physics, 1/AF, Bidhannagar, Kolkata 700064, India*
[3]*Manipal Centre for Natural Sciences, Manipal University, Manipal 576104, India*
[4]*Department of Physics, IIT Bombay, Powai, Mumbai 400076, India*
(Received 17 June 2016; published 8 September 2016)

Effects of nuclear mean field and of multiple preequilibrium (PEQ) emission on double differential neutron multiplicity distribution from heavy ion reactions ($^{12}C+^{165}Ho$ and $^{20}Ne+^{165}Ho$) at 10–30 MeV/u have been investigated in the framework of the semiclassical formalism for heavy ion reaction (henceforth termed "HION") developed earlier. HION follows the equilibration of a target+projectile composite system through the kinematics of two-body scattering. In the present work nuclear density distribution in the composite system is estimated in the relativistic mean field (RMF) approach. The nucleon-nucleon collision rates and subsequently the nucleon emission probability are calculated from this density distribution. A second approach based on a semiphenomenological formalism is also used for nuclear density distribution. Energy-angle distribution of neutron multiplicities calculated with this modified HION model coupled with multiple PEQ emission could reproduce the measured data of earlier workers in the projectile energy range of 10–30 MeV/u.

DOI: 10.1103/PhysRevC.94.034607

I. INTRODUCTION

Emission of light particles from heavy ion reactions in the energy range of a few tens of MeV/u has gained interest in the last few decades [1–3]. In heavy ion collisions (HICs) in this energy range, it has experimentally been observed that the yield of energetic nucleons and light particles is higher than is expected from the prediction of the evaporation model [4]. These emissions, which take place due to the partial energy sharing during the initial stages of compound nucleus formation and its evolution towards equilibration, are the preequilibrium (PEQ) emissions and precede evaporation emission from an equilibrated compound nucleus. In heavy ion reaction at several tens of MeV/u, along with the PEQ emissions, a few more processes such as incomplete fusion, deep inelastic collisions, and breakup fusions also play dominant roles over the former processes depending upon the particle energy [5–8]. In heavy ion reaction, the relaxation process is influenced by the nuclear mean field as well as the nucleon-nucleon interaction [9]. At a projectile energy range of ∼10–30 MeV/u, both these processes play important roles and govern the yield and energy-angle distribution of the emitted particles. A number of phenomenological and theoretical proposals [10–23] have been put forward to explain the energy-angle distribution of emitted particles at low to intermediate energy range of HIC but the issue is not yet resolved satisfactorily. The moving source parametrization [10], Fermi-jet model [11,12], exciton model [2,13–15], time dependent Hartree-Fock model [16,17], quantum molecular dynamics (QMD) calculation [18,19], Boltzmann-like transport equations and different types of Vlasov equations [20–23], and other models have been examined for the purpose.

Among these, the moving source parametrization fits the experimental spectra at different projectile energies based on the proper parametrization of the data, although the physical basis for choosing these parameters is still a point of debate. The Fermi-jet model fails to explain the experimental observation by underpredicting the measured data. The dynamical models such as the QMD and Boltzmann-like transport models are successful in the higher energy regime of nuclear reactions. These models estimate the reaction dynamics through the time evolution of nucleons considering the nucleon-nucleon (N-N) interaction in the phase space volume. We had developed a semiclassical formalism [24,25] (henceforth termed the "HION" model) to describe energy-angle distribution of preequilibrium (PEQ) nucleon emission in heavy ion reaction in the projectile energy range of 10–30 MeV/u. In this model, energy and momentum of the scattered nucleon is determined from the kinematics of nucleon-nucleon scattering. The phase space available to the excited nucleons at the onset of heavy ion fusion is determined from the overlap of Fermi momentum spheres of the two interacting nuclei. This model had certain shortcomings [24,25] in explaining the experimental double differential neutron multiplicities [26–28] in two respects. The model underestimated the experimental spectra for intermediate emission energies at the forward angle and overestimated the spectra at the backward angles. This may be attributed to the fact that in the beam energy range of 10–30 MeV/u both the two-body interaction and the nuclear mean field have a significant contribution in determining the nucleon emission cross section. Therefore a combination of the mean field effect and N-N collision can provide a better estimate of the neutron emission probabilities for heavy ion reaction in the energy range of 10–30 MeV/u. In order to investigate the influence of the mean field, and to overcome the shortcomings of the previous model, in the present study, two modifications have been incorporated in the model. Firstly, nucleon density distribution is determined using the relativistic mean field (RMF) approach [29,30] which in turn is used to estimate the emission probabilities for

*maitreyee.nandy@saha.ac.in

neutrons. The resulting emission probability is lower than that considered in the earlier version of the model from an empirical expression given by Blann [31] and helps to account for the overestimations at backward angles. A second method using a semiphenomenological approach [32,33] is also used to calculate the nucleon density distribution and the nucleon emission probability and compare with those obtained the RMF approach. Secondly, in order to account for the underestimation of the measured data by the calculated multiplicity distribution at the intermediate energies at forward angle emissions, the PEQ emissions from multiple stages are considered [34]. The brief description of the model and details of the formalism are given in the next sections. Influence of mean field in PEQ neutron emission was also investigated in an earlier work by Brusati *et al.* [35], but they had studied the angle integrated energy distribution in the framework of the microscopic Vlasov-Uehling-Uhlenbeck (VUU) model and followed the time evolution of the system. We have followed in this work the semiclassical approach and analyzed the neutron angular distribution.

The old version of the semiclassical formalism [24] (the HION model) is described in the next section, and the modifications introduced to study the effect of the mean field and that of multiple PEQ emission are presented in Sec. III. In Sec. IV we give the results of our study followed by the conclusion in Sec. V.

II. DESCRIPTION OF THE MODEL

In this work, influence of nuclear mean field and of multiple preequilibrium emissions on the energy-angle distribution of PEQ neutron emission from heavy ion reactions in the energy range of 10–30 MeV/u has been studied. This estimation is based on the semiclassical formalism [24] developed earlier by our group (the HION model and code). In order to study the two effects mentioned above, modifications have been incorporated in the model. The formalism [24] calculates the PEQ contribution until the excited composite system attains a thermodynamic equilibrium through N-N interactions. The energy and angular distribution are determined from the kinematics of two-body scattering. In the HION model for heavy ion reaction, the excited system can be formed even before the onset of any two-body interaction. This initial excited configuration of the composite system is modeled through overlap of the Fermi momentum sphere of the projectile and target nucleus which is described in detail in [24]. The PEQ double differential cross section for an ejectile of type ν is given by [24]

$$\frac{d^2\sigma^\nu}{d\varepsilon d\Omega} = \sigma_{\rm fus} \sum_N f_N^\nu \left[\frac{\lambda_C^\nu(\varepsilon)}{\lambda_C^\nu(\varepsilon) + \lambda_t^\nu(\varepsilon)} \right] P_N(\varepsilon,\Omega). \quad (1)$$

Here, $\sigma_{\rm fus}$ represents the absorption cross section of a projectile particle in the target nucleus. The summation starts from $N = 0$ (before any two-body interaction starts) and extends until equilibration is reached [24]. The probability of the emitted particle being in the energy range ε and $\varepsilon + d\varepsilon$ and solid angle Ω and $\Omega + d\Omega$ is $P_N(\varepsilon,\Omega)d\varepsilon d\Omega$. This probability is related to the energy-angle distribution of the ejectile within the nucleus obtained from scattering kinematics and to the effect of refraction at the nuclear surface. The term in the square bracket provides the probability of emission of the ν-type particle with energy ε. $\lambda_C^\nu(\varepsilon)$ and $\lambda_t^\nu(\varepsilon)$ are the rate of emission of the ν-type particle with energy ε and the rate of two-body collisions with other nucleons, respectively. f_N^ν gives the number of ν-type excited particles at the Nth two-body interaction [24].

The model considers the composite nucleus to be divided into two parts, a hot spot and a cold spot. The hot spot incorporates the effect of nuclear excitation and is defined by a finite temperature Fermi distribution, whereas the cold spot is described by a zero temperature Fermi distribution. Angular distribution of the emitted particles was obtained from the weighted sum of contributions from these two subsystems [24,36]: interaction between two nucleons in the hot spot leading to creation, annihilation, or redistribution of the particle-hole pair and interaction between a particle in the hot spot with another in the cold spot leading to creation of particle-hole pairs. The detailed description of the scattering kernels, initial number of excited particles, and energy-angle distribution can be found in [24,36].

The model in its original form [24,36] described above does not take into account any influence of the nuclear mean field in the nucleon emission probability or cross section. It calculates the two-body collision rate $\lambda_t^\nu(\varepsilon)$ using an empirical formalism of Blann [31] as given by

$$\lambda_t^\nu(\varepsilon) = \frac{[1.4 \times 10^{21}(\varepsilon + B_\nu) - 6.0 \times 10^{18}(\varepsilon + B_\nu)^2]}{k}, \quad (2)$$

where B_ν is the binding energy of the ν-type particle in the nucleus and k is an adjustable parameter taken as 1.0. The model calculates the nucleon emission rate from the cross section of the inverse reaction and considers only single PEQ nucleon emission from the target+projectile composite system. This formalism overestimates neutron emission at backward angles and underestimates neutron emission for intermediate emission energies at forward angles. The model has been modified to investigate (i) the effect of nuclear mean field on the nucleon emission probability and (ii) the influence of PEQ contribution from multiple stages on improving these shortcomings. In order to investigate the contribution of nuclear mean field, nucleon density distribution inside the nuclear matter is calculated using the relativistic mean field (RMF) approach. The nucleon-nucleon collision rates inside the nucleus are determined from this density distribution and the nucleon-nucleon scattering cross section. Subsequently the nucleon emission probability is calculated from a competition between the two-body interaction and nucleon emission rates.

III. MODIFICATIONS INCORPORATED

In heavy ion collisions in the energy range of tens of MeV/u to a few hundred MeV/u, nucleon-nucleon interactions play a leading role in the excitation and deexcitation phase of the nuclear reaction. The matter density distribution within the nucleus determines the nucleon mean free path which strongly influences the total interaction rate and angular distribution of scattering. Density distribution inside the nucleus is pre-

dominantly determined from the prevalent nuclear field. In the present study, the influence of this nuclear mean field, resulting nuclear density distribution, and that of multiple emissions from the PEQ stage of the relaxation process in the context of neutron emission have been investigated. Multiple preequilibrium emissions of nucleons from the first composite and first residual (formed after particle emission from the composite) nuclei have been included in the model in an attempt to improve the agreement of the calculated nucleon multiplicity with the experimental data.

A. Nucleon density distribution

In the previous form of the model HION, an empirical expression (2) for two-body collision rates given by Blann [31] was used to estimate the emission probability [the term in the square brackets of Eq. (1)]. In the present work, in order to analyze the mean field effect on the relaxation process and on particle emission, nucleon density distribution of the composite nucleus for the reactions under study is determined in the framework of RMF [29,30] theory. A second approach—the semiphenomenological model [32,33]—is also adopted for the calculation of nucleon density distribution in order to have a comparison with the results of the RMF approach. As central and near central collisions are considered for comparison with experimental data, the nucleon mean free path is determined from the density distribution at different impact parameters for small values of the angular momentum ℓ.

Two-body collision rates inside the nuclear matter and subsequently the neutron emission probabilities are calculated from the nucleon mean free path so obtained. The emission probabilities calculated in this method replaced the emission probabilities calculated from the empirical expression for two-body collision rates [31] in the old model. Total nucleon multiplicity has been determined as the weighted sum of the multiplicities for the reaction taking place at different impact parameters. The effective nuclear excitation ($E^*_{\rm eff}$) at each impact parameter ℓ has been modified to take into account the rotational energy ($E_{\rm rot}$) losses. The effective excitation energy available for reaction is given by

$$\begin{aligned} E^*_{\rm eff} &= E_{\rm CM} - E_{\rm rot}, \quad \text{and} \\ \mathrm{E}_{\rm rot} &= [\ell(\ell{+}1)\hbar^2]/(2\mu R^2), \end{aligned} \tag{3}$$

where $E_{\rm CM}$ is the center-of-mass energy and R is the radius of the composite nucleus. In the following subsections, a brief description is presented for the calculation of the density distribution, emission probabilities, and multiple preequilibrium neutron emission to obtain the energy-angle distribution of the preequilibrium contribution.

1. Relativistic mean field approach

The relativistic mean field (RMF) or the density functional approach starts with a Lagrangian describing the Dirac spinor nucleons interacting via the meson fields. The mesons considered are the scalar σ, the vector ω, and the isovector ρ, in addition to the photon. The σ meson provides a strong attraction whereas the ω meson provides strong repulsion, such that the sum (attraction+repulsion) of σ and ω contributions roughly adds up to around 50 MeV, the value consistent with the accepted nonrelativistic value of the average nucleon potential inside the nucleus. The inclusion of the ρ meson accounts for the small isospin dependence. The variation principle yields the equations of motion. At this stage the mean field approximation is introduced. As a result the fields are not quantized and so are replaced by c numbers (the expectation values). This along with the time reversal invariance leads to the Dirac-type equation with potentials involving the meson fields describing the nucleons and Klein-Gordon-type equations with sources involving the nucleon currents and densities for mesons. This nonlinear set of coupled equations, known as RMF equations, are to be solved self-consistently. The required set of parameters appearing in the Lagrangian is usually determined through the χ^2 fit to reproduce the observed ground state properties of a few selected spherical nuclei. The fit is not unique. Several sets of parameters exist; some of these even include additional coupling terms and/or additional mesons. Here, the basis expansion method with axially deformed oscillator basis is used to solve the RMF equations and the most widely used Lagrangian parameter set NL3 [37] is employed. This parameter set is then frozen and is used in the calculation for any nucleus. The calculation yields the nucleon spinors, total binding energy (BE), and the deformation. Other observables like the proton and neutron rms radii, neutron skin, nucleon density distributions, quadrupole moments, etc., can then be calculated. The resulting axially deformed (function of r and θ) density distributions are expanded in terms of multipoles and the $L = 0$ (spherical) part is projected out. This spherical part with correct normalization is used in the present work. For details see Ref. [29].

2. Semiphenomenological approach

In the semiphenomenological approach [32,33], which incorporates correctly the behavior at the center ($r \to 0$) and the behavior at $r \to \infty$ (asymptotic), the nucleon density distribution is written as

$$\begin{aligned} \rho_i(r) &= \frac{{\rho_i}^0}{1+\beta_i\left[1+\left(\frac{r}{R}\right)^2\right]^{\alpha_i}\left[e^{(r-R)/a_i}+e^{-(r+R)/a_i}\right]}; \\ a_i &= \frac{\hbar}{2(2mE_i)^{1/2}}, \quad \alpha_i = \frac{q}{\hbar}\left(\frac{m}{2E_i}\right)^{1/2}+1, \quad \text{and} \\ \beta_i &= 2^{-\alpha_{ii}}. \end{aligned} \tag{4}$$

$i = n$ (neutron) or p (proton); E_i is the corresponding separation energy of i-type nucleon; $q = 0$ for neutrons and $q = Z - 1$ for protons, Z being the atomic number. The parameters ${\rho_n}^0$, ${\rho_p}^0$ are determined through the normalization over the total neutron and proton numbers; R, the lone parameter left, is estimated by reproducing the experimental rms charge density radius. The same value of R is used for neutrons. A detailed description can be found in [33].

B. Calculation of the emission probability

The emission probability is calculated from a competition between N-N collision rate $\lambda^\nu_I(\varepsilon)$ and nucleon emission rate $\lambda^\nu_C(\varepsilon)$. The emission rate $[\lambda^\nu_C(\varepsilon)]$ of the ν-type particle from

the composite nucleus at energy (ε) is given as [38]

$$\lambda_C^{\nu}(\varepsilon) = \frac{(2S_\nu + 1)m_\nu \varepsilon \sigma_{inv}(\varepsilon)}{\pi^2 \hbar^3 g}, \quad (5)$$

where S_ν and m_ν are the spin and mass of the ν-type particle, σ_{inv} is the cross section for the reverse reaction, and g is single particle level density. σ_{inv} is calculated using the method of Chatterjee *et al.* [38]. As mentioned earlier, in the previous version of the model HION, $\lambda_t^{\nu}(\varepsilon)$ was determined from the empirical relation [Eq. (2)] given by Blann [31]. In the present work a more realistic approach has been adopted. The rate of two-body collisions has been estimated from the exciton velocity within the nucleus and the corresponding mean free path (λ). λ inside the nucleus is determined from the energy dependent N-N interaction cross sections [39] and the matter density distribution. Nucleon mean free path (λ) is given by the relation

$$\lambda = \frac{1}{\rho\sigma}. \quad (6)$$

Here the mean nucleon density distribution $\rho = \rho_n + \rho_p$; σ is the weighted sum of the N-N cross sections, σ_{nn},σ_{np}, respectively, and is given by

$$\sigma = \frac{N}{A}\sigma_{nn} + \frac{Z}{A}\sigma_{np}. \quad (7)$$

ρ_n, ρ_p, and subsequently ρ are calculated using Eq. (4) for the semiphenomenological approach and the RMF approach using the method of Gambhir *et al.* [29]. σ_{nn} and σ_{pp} are calculated using the formalism of Charagi and Gupta [39].

C. Multiple preequilibrium (PEQ) emission

In the older version of the model single particle emission from the target+projectile composite system only was considered throughout the equilibration processes. This approach underestimated the experimentally measured neutron multiplicities for intermediate emission energies at forward angles in the case of ^{20}Ne + ^{165}Ho reaction at 30 MeV/u and in the case of ^{12}C + ^{165}Ho reaction at 25 MeV/u [26–28]. In order to improve the agreement of the calculated results with the measured data, a multiple preequilibrium prescription has been introduced in the study. Multiple PEQ emission is possible when the incoming particle has sufficient energy which can knock off more than one particle from the fused system, before attaining a thermal equilibrium, so multiple PEQ emission from a system is expected in the first few exciton hierarchies when the average energy per particle is large. In our work, we have considered two possible ways of multiple PEQ emission: (i) simultaneous two neutron PEQ emission—more than one neutron is emitted from a single exciton hierarchy and (ii) PEQ emission from successive stages–PEQ emission from different exciton hierarchies. In these two cases, the formalisms differ significantly considering the emission of particles from two different sets of originating nuclei. In the former case, the particles are emitted from the same exciton state of the nonequilibrated (target+projectile) composite system leading to a residual nucleus with a mass number A-2, so for the "simultaneous" case, from an exciton hierarchy all particle emission probabilities and the kinetic energy distribution of the emitted particles were estimated considering the system excitation energy of the initial nucleus. The probability that both the particles are emitted with the same emission energy ε in the direction ω from the same exciton state of the composite system is given by the combined probability of the two single particle emissions (Blann and Vonach [34]). Thus the probability $P_{nn}(\varepsilon,\omega)$ that two neutrons each with energy ε are emitted in the direction ω from the same exciton hierarchy is given by $P_{nn}(\varepsilon,\omega) = P_n(\varepsilon,\omega)P_n(\varepsilon,\omega)$, where $P_n(\varepsilon,\omega)$ is the probability of single neutron emission.

On the contrary, in the case of sequential PEQ process from two successive stages, emission in the second stage takes place from the residual system with mass number A-1 generated after the first particle emission from the (target+projectile) composite system. This residual nucleus (A-1) is at a lower excitation energy $E_c' = E_c - \varepsilon$ where ε is the emission energy of the first particle. PEQ particles emitted from this stage may carry an energy in the range $0 - (E_c - \varepsilon)$. Thus for a given projectile energy, the probability of intermediate energy multiple PEQ increases more through sequential process than that of high energy emissions. The total probability of PEQ neutrons emitted with energy angle (ε, ω) from two successive stages is obtained from the sum of the PEQ emission probabilities from the composite system and the first residual with mass number (A-1). It is given by

$$\frac{d^2\sigma^{\nu}}{d\varepsilon d\Omega} = \sigma_{\text{fus}} \sum_{N,i} f_{N,i}^{\nu} \left[\frac{\lambda_C^{\nu}(\varepsilon)}{\lambda_C^{\nu}(\varepsilon) + \lambda_i^{\nu}(\varepsilon)} \right] P_{N,i}(\varepsilon,\Omega), \quad i = 1,2. \quad (8)$$

In calculating the above probability as a sum of emission probabilities from the two nuclei from different interaction stages, we have considered the probability of *N*th interaction in a nucleus to occur without prior emission [24]. This formalism excludes the possibility of repeated counting from the same system.

D. Calculation of the evaporation neutrons

The evaporation neutron multiplicities are calculated using the Monte Carlo procedure for estimating the decay mode of the excited nucleus in the framework of Hauser-Feshbach formalism. The projection angular momentum coupled evaporation code, PACE4 [40,41] has been used for this purpose. In the code, the deexcitations are solely governed by the height of the fission barrier and level densities of the excited nucleus. In the present version of the code PACE4, the fusion cross sections are estimated using the Bass model [42], the optical model parameters for nucleons and alpha particles are taken from [43], and the level densities are derived using the Fermi gas formalism. In the present study, the level density parameter has been chosen to be A/10 and angular distribution of the emitted neutron multiplicities is estimated to account for the evaporation contributions of the systems under study.

IV. RESULTS AND DISCUSSION

In this work we have studied the effect of nuclear mean field through the resulting nucleon density distribution and that of multiple PEQ emission on the energy-angle distribution

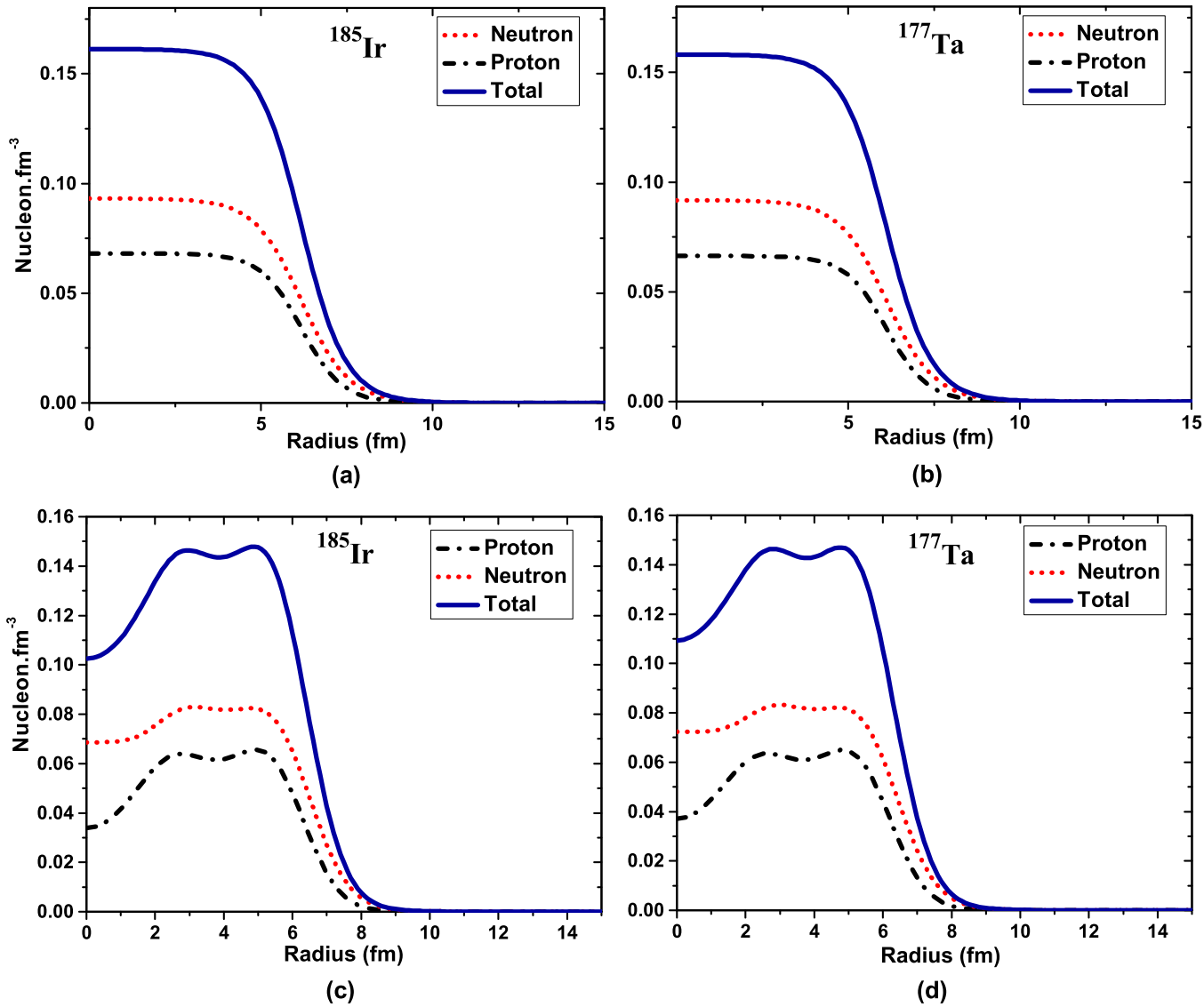

FIG. 1. Nucleon density distribution for both compound nuclei ^{185}Ir (^{20}Ne + ^{165}Ho) and ^{177}Ta (^{12}C + ^{165}Ho) systems using the semiphenomenological approach (a,b) and the RMF approach (c,d).

of neutrons from two reaction systems: ^{20}Ne + ^{165}Ho and ^{12}C + ^{165}Ho at different projectile energies. The composite systems formed in these two reactions are ^{185}Ir and ^{177}Ta, respectively. The nucleon density distributions for ^{185}Ir and ^{177}Ta using RMF and semiphenomenological approaches are shown in Fig. 1. The semiphenomenological approach shows a near constant nucleon density in the central part of the nucleus with a larger density of neutrons in the range of 0.093 and 0.092 fm^{-3}, whereas the proton densities are found to be 0.068 and 0.066 fm^{-3} for ^{185}Ir and ^{177}Ta, respectively.

In contrary to the above observation, the RMF approach shows a distinctly different density distribution of the nucleons in the compound nucleus. In both the cases, the central density is found to be less compared to the maximum density around $r \sim 3.0$ fm and $r \sim 5.0$ fm. In the case of neutrons the central density is found to be 83% of the maximum density and the nucleon density appears as a double hump in the range of 3–5 fm with a small dip at 4 fm. A similar but more pronounced trend is found in the case of the proton densities; the central density is found to be around half of the maximum density. The collective nucleon density distribution shows, at the center, a density of 70% of the maximum value at 5.0 fm.

From the calculated density profile and associated in medium N-N interaction cross sections as obtained from [38,39], the two-body collision rates and subsequently the emission probabilities of neutrons are calculated as a function of neutron energy for different values of ℓ for both the composite systems. These emission probabilities for $\ell = 10$ are shown in Fig. 2 along with that calculated using the N-N collision rate given by Eq. (2). For both ^{185}Ir and ^{177}Ta, a higher emission probability is obtained from the RMF approach for nucleon density distribution compared to the semiphenomenological model. The variation is energy dependent and increases with increase in the emission energy of the neutrons. For the ^{20}Ne + ^{165}Ho system with semiphenomenological approach of density distributions, the

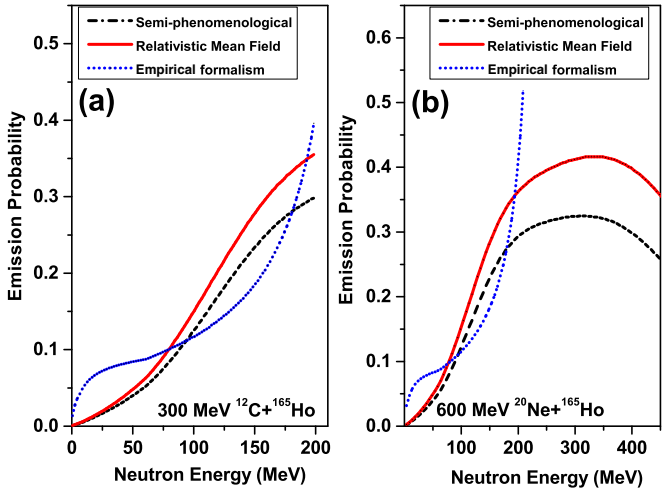

FIG. 2. Comparison of the emission probabilities obtained with the semiphenomenological and RMF approach for the $^{12}C+^{165}Ho$ and $^{10}Ne+^{165}Ho$ system for $\ell = 10$. Also shown in the figure is neutron emission probability calculated from a competition between the collision rate given by Eq. (2) and the emission rate given by Eq. (5).

emission probabilities increase up to 0.32 at emission energy 260 MeV, maintain a plateau up to 350 MeV, and then decrease at higher emission energies. A similar kind of initial increase and further decreasing pattern in the emission probabilities is observed in the RMF approach as well—the emission probabilities increase until 0.42 and then reduce at higher emission energies. In the case of the $^{12}C+^{165}Ho$ system at 300 MeV, the emission probability is found to be higher with RMF approach, and monotonically increases. Moreover, the nucleon emission probability calculated from density dependent collision rates is lower than that obtained from the empirical formalism of Blann [31] [Eq. (2)]. The variation is more pronounced at lower neutron energies as the empirical formalism shows weak energy dependence.

Using the N-N collision rate and the emission probabilities described above, the PEQ contribution to neutron multiplicities are calculated using Eq. (1) for the reaction systems considered. The total energy-angle distribution of neutron multiplicities is calculated as a sum of PEQ and evaporation contribution. In Figs. 3(a) 3(b), and 4(a)–4(c) we have compared the PEQ contribution to neutron multiplicities calculated from the RMF and the semiphenomenological approach (henceforth termed "HION2" and "HION3," respectively) with the experimental measurements for $^{20}Ne+^{165}Ho$ reaction at different beam energies. Also shown in these figures are the results obtained from the old version of HION (henceforth termed "HION1") code, some of which have already been reported [24]. In Fig. 5 we have given a similar comparison for the $^{12}C+^{165}Ho$ reaction at 300 MeV.

The experimental measurements are shown as black circles and the associated statistical uncertainties with error bars; diamond represents the HION1 formalism, solid and dotted lines characterize the HION results with RMF density (HION2) and those with semiphenomenological density distributions (HION3), respectively. The dashed line gives

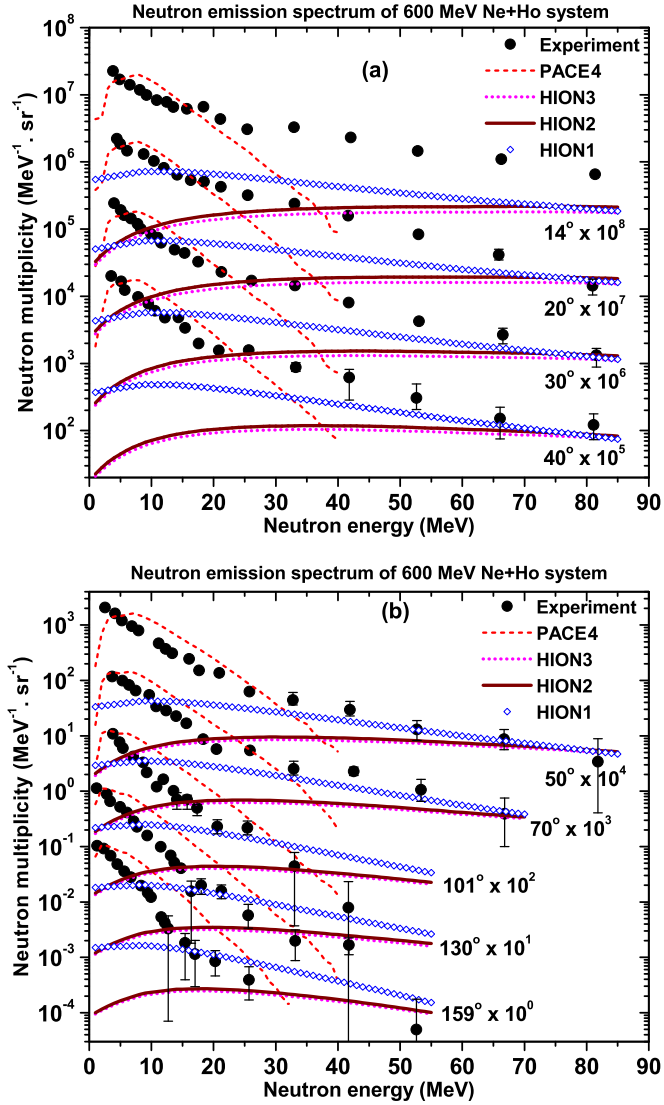

FIG. 3. Comparison between the experimentally obtained (black circles with error bars) and theoretically calculated neutron multiplicities (evaporation from PACE4, PEQ from HION model): (i) dashed line: PACE4; (ii) diamond: HION1; (iii) solid line: HION with RMF approach (HION2); (iv) dotted line: HION with semiphenomenological approach (HION3) for $^{20}Ne+^{165}Ho$ reaction at 600 MeV.

the evaporation contribution calculated with the PACE4 code. From Fig. 3 we observe that, for 30 MeV/u $^{20}Ne+^{165}Ho$, at angles 20°–70° results from the old formalism (HION1) show good agreement with the experimental data for PEQ contribution at the higher end of the neutron emission range. However, HION1 calculations underestimate the measured multiplicity at intermediate emission energies at 14° and 20°. Moreover, these calculations overestimate the experimental data at backward angles for higher neutron energies and the disagreement increases as one moves away from the incident beam direction [101°, 130°, 159° in Fig. 3(b)]. For ^{20}Ne induced reaction on ^{165}Ho at 402, 292, and 220 MeV (Fig. 4), the neutron multiplicities calculated with HION1 closely match the measured spectra for PEQ emission at

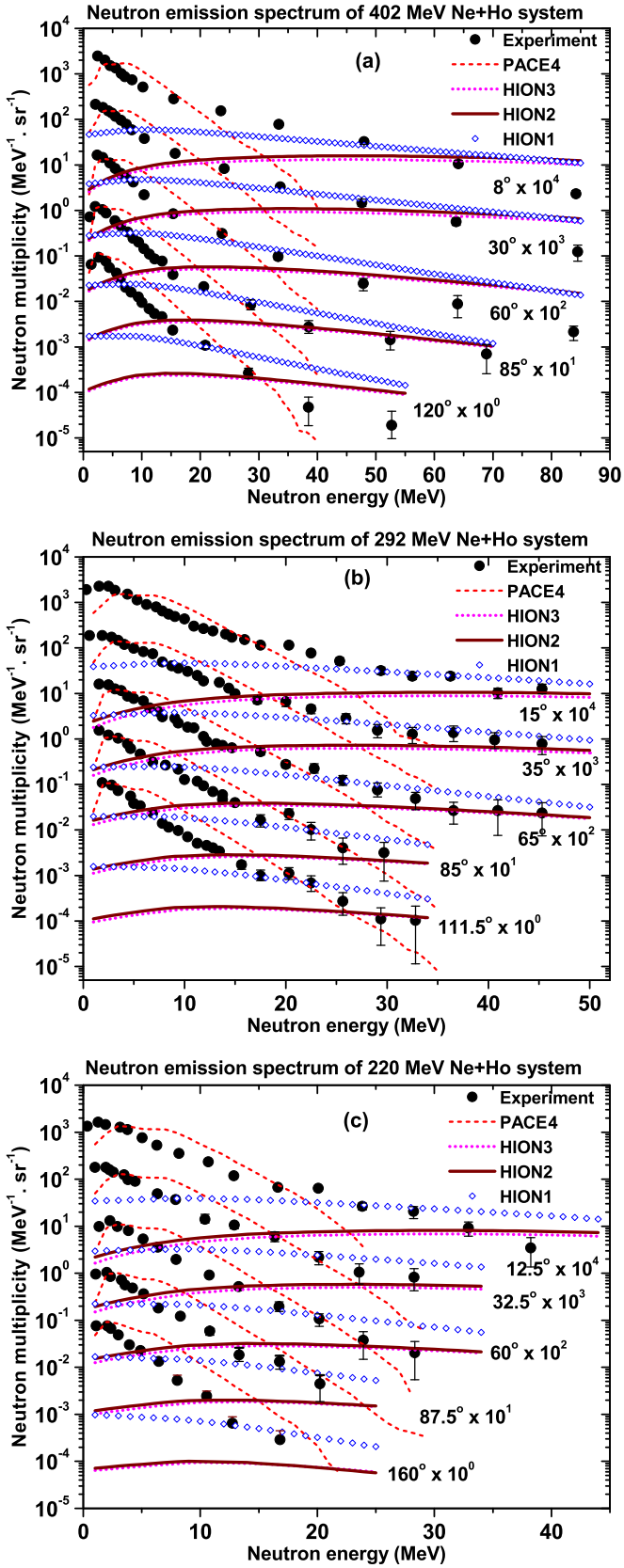

FIG. 4. Comparison between the experimentally obtained (black circles with error bars) and theoretically calculated neutron multiplicities (evaporation from PACE4, PEQ from HION model): (i) dashed line: PACE4; (ii) diamond: HION1; (iii) solid line: HION2); (iv) dotted line: HION3 for ^{20}Ne + ^{165}Ho reaction at (a) 402 MeV, (b) 292 MeV, and (c) 220 MeV.

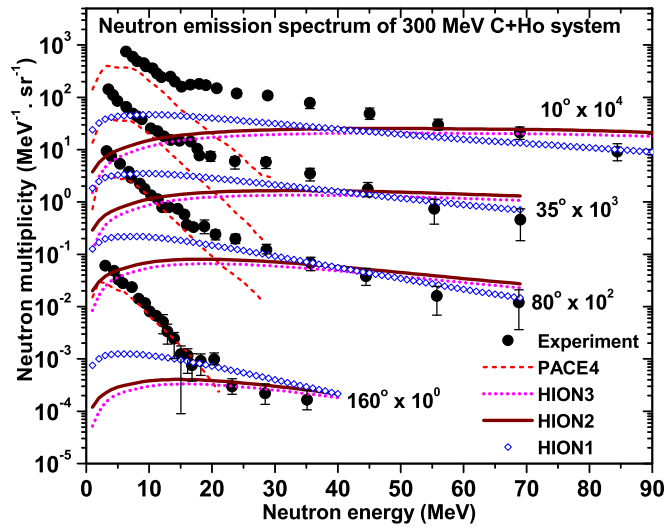

FIG. 5. Comparison between the experimentally obtained (black circles with error bars) and theoretically calculated neutron multiplicities (evaporation from PACE4, PEQ from HION model): (i) dashed line: PACE4; (ii) diamond: HION1; (iii) solid line: HION with RMF approach (HION2); (iv) dotted line: HION with semiphenomenological approach (HION3) for ^{12}C + ^{165}Ho reaction at 300 MeV.

the forward angles (at neutron energies above 30–35 MeV evaporation contribution is negligible and the measured data represent solely the PEQ contribution) but overestimation of the calculated neutron multiplicity at backward angles persists. In the case of ^{12}C + ^{165}Ho at 25 MeV/u, shown in Fig. 5, the calculated PEQ spectrum with HION1 at 10° underestimates the measured distribution between 15 and 50 MeV. In order to resolve this mismatch between the calculated and measured PEQ neutron emission and to analyze the influence of the nuclear mean field, nucleon density distribution of the composite systems ^{177}Ta and ^{185}Ir, obtained from RMF calculations, has been introduced to estimate the two-body collision rates in the present study. A second approach using the semiphenomenological formalism [32] is also used to determine the density distribution and the collision rates. Neutron emission probabilities as a function of neutron energy are then determined from a competition between these collision rates and the neutron emission rates. Neutron multiplicities calculated with this modified approach are also shown in Figs. 3–5 for ^{20}Ne and ^{12}C induced reactions, respectively, on the ^{165}Ho target.

The new approach has reduced the neutron multiplicities compared to the earlier results as the emission probability decreases as compared to that obtained from the empirical formalism [Eq. (2)]. This decrease is more at lower emission energies which is also reflected in the neutron multiplicity. As a result the PEQ contribution calculated from RMF (hence-

forth termed "HION2") and from the semiphenomenological approach (henceforth termed "HION3"), at backward angles agrees well with the measured data. For the ^{20}Ne + ^{165}Ho reaction at 600 MeV the calculated PEQ neutron multiplicity at forward angles largely underpredicts the experimental data for neutron energies higher than 30 MeV. In the case of 402 MeV ^{20}Ne on ^{165}Ho the calculated PEQ neutron multiplicity matches significantly well with the measured data at the backward angles 30° onwards compared to the earlier estimates as shown in Fig. 4. Similar observations have also been found for 292 and 220 MeV beam energies. For the last two cases the backward angle estimates are much better reproduced with the new approach. For 292 MeV projectile energy, in the extreme forward angle at high emission energy the present study has shown a better corroboration with respect to the measurements. At the backward angles, the present calculations complement better with the experimental measurements. Similarly for 220 MeV incident energy, the overestimation of the HION1 results have been improved with both HION2 and HION3 calculations for backward angles. At 160° emission angle the variation is less between the HION1 and the corresponding new approach due to very small contribution of the preequilibrium emissions.

Similar results were found in the case of the ^{12}C + ^{165}Ho system. From Fig. 5 we observe that HION1 calculations underpredict the measured neutron multiplicity at 10° and at 35° for neutron energies above 16–18 MeV where the PEQ contribution plays an important role. HION1 results overestimate the experimental data at 160° above 18 MeV emission energy. In these emission energy ranges the PEQ contribution predominates the neutron emission. Neutron multiplicity calculated for this system using RMF and semiphenomenological density distribution and the subsequent density dependent N-N collision rate (HION2, HION3) further underestimates the intermediate energy emissions at forward angles as shown in Fig. 5. This decrease in the calculated neutron multiplicity is due to the lower emission probability as compared to the calculations with HION1, but the reduction in emission probability results in a better agreement of the calculated and measured multiplicities at backward angles. Our analysis for ^{20}Ne induced reactions at different beam energies shows that the overprediction of the calculated results for low neutron emission energies is attributed to the overprediction of evaporation contribution as predicted by the PACE4 code. In the case of a ^{12}C induced reaction PACE4 results predict the neutron multiplicity at low emission energy fairly well.

In order to account for the underestimation of the experimental results by the present formalism (HION2 and HION3) for intermediate energy emissions at forward angles we have investigated the contribution of PEQ emission from multiple stages to forward angle emission. In the next stage of the present work we have calculated the multiple PEQ emission—(i) "simultaneous," from the first composite nucleus, and (ii) "successive," from the first composite as well as from the first residual (after single PEQ emission from the composite system) nucleus. It has been observed from our study that for the reaction systems considered the first process contributes at most 2%–3% of the total PEQ while the contribution of the second process is about 40% of the total PEQ emission. This

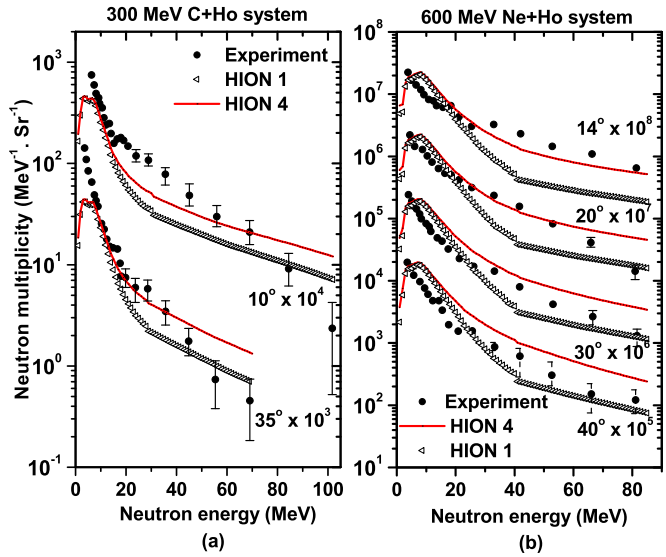

FIG. 6. Comparison between the experimental and theoretically obtained [evaporation contribution from the PACE4 code, preequilibrium from (i) HION1 model (triangle), (ii) HION2+simultaneous and sequential (from successive stages) multiparticle emission (HION4) (solid line)] neutron multiplicities at different angles at (a) 300 MeV for ^{12}C + ^{165}Ho system and (b) 600 MeV for ^{10}Ne + ^{165}Ho system.

is because when we consider PEQ emission from successive stages, single PEQ emission from the residual nucleus has also been taken into account. The calculated results for the total PEQ multiplicity (RMF approach+multiple PEQ, henceforth termed "HION4") at forward angles are compared with the experimentally measured data and the calculations from HION1 in Fig. 6. Neutron emission at 10° and 35° emission angles from ^{12}C + ^{165}Ho at 300 MeV and at 14°, 20°, 30°, and 40° emission angles from the ^{20}Ne + ^{165}Ho reaction at 600 MeV, respectively, are shown in this figure. From this comparison we see that the multiple PEQ emission can predict the measured neutron emission quite well at 14° and 20° for 600 MeV ^{20}Ne + ^{165}Ho. At 30° and 40° emission angle multiple PEQ results in a slightly higher neutron emission compared to the measured data. In the case of the 300 MeV ^{12}C induced reaction on ^{165}Ho multiple PEQ emission helps to improve the agreement with the measured neutron emission at the forward angle. Thus it is observed that for the projectile energies considered in this work, the multiple PEQ mechanism plays an important role in forward angle emission of neutrons.

We have calculated the angular variation of the PEQ contribution, obtained from HION calculations, in the total neutron yield for the ^{20}Ne and ^{12}C induced reaction on ^{165}Ho Table I shows the PEQ contribution as a percentage of the total yield at different angles of emission for 600 and 402 MeV ^{20}Ne + ^{165}Ho and 300 MeV ^{12}C + ^{165}Ho. From Table I we observe that for a given projectile energy the PEQ contribution decreases as we move to backward angles. As beam energy increases the forward angle emissions increase significantly which is also a signature of PEQ reaction. Significantly higher PEQ emission at forward angles compared to the backward angles in the case of ^{20}Ne + ^{165}Ho at 600 MeV and ^{12}C + ^{165}Ho

TABLE I. Percentage contribution of PEQ emission at different angles.

Reaction	Beam energy (MeV)	Angle (°)	PEQ emission (%)
^{20}Ne + ^{165}Ho	402	8	5.7
		30	4.2
		60	2.3
		85	1.6
		120	1.2
	600	14	33.9
		20	33.0
		30	32.7
		40	31.9
		50	3.18
		70	2.22
		101	1.51
		130	1.47
		159	1.23
^{12}C + ^{165}Ho	300	10	47.7
		35	40.4
		80	12.4
		160	6.0

300 MeV may be attributed to the fact that the multiple PEQ mechanism plays an important role in neutron emission at forward angles for these reactions.

V. CONCLUSION

In the present work, we have studied the effects of nuclear mean field and of emission from multiple stages on the energy-angle distribution of PEQ emission of neutrons in heavy ion reactions at energies ∼10–30 MeV/u. The reaction systems studied are the ^{20}Ne + ^{165}Ho reaction at 220, 292, 402, and 600 MeV and the ^{12}C + ^{165}Ho reaction at 300 MeV. In order to study the influence of mean field, nucleon density distribution is calculated in the framework of RMF theory. Two-body collision rates inside the nuclear matter are determined from this density distribution and the free nucleon-nucleon scattering cross section. The two-body collision rates so obtained are used to calculate the neutron emission probability. A second approach using the semiphenomenological model of Gambhir and Patil [32] is also used to calculate the density distribution and compare with the corresponding results of the RMF approach. The density distributions calculated using the RMF approach and the semiphenomenological model result in an emission probability lower than that calculated by the empirical formalism of Blann [31] up to ∼70 MeV neutron energy. The energy-angle distribution of the emitted neutrons is calculated from the kinematics of two-body scattering following the method of Nandy *et al.* [24]. Neutron multiplicity calculated from the density dependent collision rates and consequent emission probability agrees well with the experimental data at backward angles, the agreement being better than that obtained from HION1. However, for projectile energies in the range of 25–30 MeV/u single PEQ emission alone (calculated in this approach) underpredicts the forward angle emission. This underprediction is rectified when the PEQ contribution from multiple stages is incorporated (HION4). Thus the new approach in the HION model (HION4) incorporating the mean field effect and multiple PEQ emission (for forward angles at 25–30 MeV/u) can predict the neutron multiplicity distribution fairly well in the projectile energy range of 10–30 MeV/u.

ACKNOWLEDGMENTS

The authors sincerely thank Dr. T. Bandyopadhyay, Head, Accelerator Radiation Safety Section for his continuous support and involvement during the course of work. We would like to show our gratitude to Dr. R. M. Tripathi, Head, Health Physics Division and Dr. K. S. Pradeepkumar, Associate Director, Health, Safety & Environment Group, BARC for the inspiration in carrying out these studies. The authors are grateful to Dr. P. K. Sarkar, Manipal Centre for Natural Sciences, Manipal University and Ex-BARC, Mumbai for fruitful academic discussion and suggestion. One of the authors, M.N., acknowledges the support of XIIth plan project Biomolecular Assembly, Recognition and Dynamics (BARD) (Project No. 12-R&D-SIN-5.04-0103), SINP, DAE, Govt. of India for financial and infrastructural support in carrying out the work.

[1] M. Blann, Phys. Rev. C **31**, 1245 (1985).
[2] H. Machner, Phys. Rev. C **28**, 2173 (1983).
[3] J. Pal, S. Saha, C. C. Dey, P. Banerjee, S. Bose, B. K. Sinha, M. B. Chatterjee, and S. K. Basu, Phys. Rev. C **71**, 034605 (2005).
[4] A. Iwamoto, Phys. Rev. C **35**, 984 (1987).
[5] K. Hanold, L. G. Moretto, G. F. Peaslee, G. J. Wozniak, D. R. Bowman, M. F. Mohar, and D. J. Morrissey, Phys. Rev. C **48**, 723 (1993).
[6] L. F. Canto, R. Donangelo, Lia M. de Matos, M. S. Hussein, and P. Lotti, Phys. Rev. C **58**, 1107 (1998).
[7] S. Wald, I. Tserruya, Z. Fraenkel, G. Doukellis, H. Gemmeke, and H. L. Harney, Phys. Rev. C **25**, 1118 (1982); **28**, 1538 (1983).
[8] D. P. Singh, Unnati, P. P. Singh, A. Yadav, M. K. Sharma, B. P. Singh, K. S. Golda, R. Kumar, A. K. Sinha, and R. Prasad, Phys. Rev. C **80**, 014601 (2009).
[9] S. Kailas, Pramana **57**, 75 (2001).
[10] T. C. Awes, G. Poggi, C. K. Gelbke, B. B. Back, B. G. Glagola, H. Breuer, and V. E. Viola, Phys. Rev. C **24**, 89 (1981); T. C. Awes, S. Saini, G. Poggi, C. K. Gelbke, D. Cha, R. Legrain, and G. D. Westfall, *ibid.* **25**, 2361 (1982).
[11] J. P. Bondrof, J. N. De, A. O. T. Karvinen, and B. Jakobsson, Nucl. Phys. A **333**, 285 (1980).
[12] J. Randrup and R. Vandenbosch, Nucl. Phys. A **474**, 219 (1987); S. Bhattacharya, K. Krishan, S. K. Samaddar, and J. N. De, Phys. Rev. C **37**, 2916 (1988).
[13] M. Blann, Phys. Rev. C **23**, 205 (1981).

[14] T. Otsuka and K. Harada, Phys. Lett. B **121**, 106 (1983).
[15] S. Yoshida and H. Morinaga, Z. Phys. A **317**, 173 (1984).
[16] A. S. Umar, M. R. Strayer, D. J. Ernst, and K. R. Sandhya Devi, Phys. Rev. C **30**, 1934 (1984).
[17] H. S. Koller, Nucl. Phys. A **438**, 564 (1984).
[18] J. Achelin, Phys. Rep. **202**, 233 (1991).
[19] K. Niita, S. Chiba, T. Maruyama, T. Maruyama, H. Takada, T. Fukahori, Y. Nakahara, and A. Iwamoto, Phys. Rev. C **52**, 2620 (1995); K. Niita, T. Maruyama, T. Maruyama, and A. Iwamoto, Prog. Theor. Phys. **98**, 87 (1997).
[20] H. Kruse, B.V. Jacak, J. J. Molitoris, G. D. Westfall, and H. Stocker, Phys. Rev. C **31**, 1770 (1985).
[21] G. Bertsch and S. Dasgupta, Phys. Rep. **160**, 189 (1989).
[22] C. Gregoire, B. Remand, F. Sebille, L. Vinet, and Y. Raffray, Nucl. Phys. A **465**, 317 (1987).
[23] A. Bonasera, F. Gulminelli, and J. Molitoris, Phys. Rep. **243**, 1 (1994).
[24] M. Nandy, S. Ghosh, and P. K. Sarkar, Phys. Rev. C **60**, 044607 (1999).
[25] P. K. Sarkar and M. Nandy, Phys. Rev. E **61**, 7161 (2000).
[26] D. Hilscher, H. Rossner, A. Gamp, U. Jahnke, B. Cheynis, B. Chambon, D. Drain, C. Pastor, A. Giorni, C. Morand, A. Dauchy, P. Stassi, and G. Petitt, Phys. Rev. C **36**, 208 (1987).
[27] E. Holub, D. Hilscher, G. Ingold, U. Jahnke, H. Orf, and H. Rossner, Phys. Rev. C **28**, 252 (1983).
[28] E. Holub, D. Hilscher, G. Ingold, U. Jahnke, H. Orf, H. Rossner, W. P. Zank, W. U. Schroder, H. Gemmeke, K. Keller, L. Lassen, and W. Lucking, Phys. Rev. C **33**, 143 (1986).
[29] Y. K. Gambhir, P. Ring, and A. Thimet, Ann. Phys. **198**, 132 (1990).
[30] P. Ring, Prog. Part. Nucl. Phys. **37**, 193 (1996).
[31] M. Blann, Phys. Rev. Lett. **27**, 337 (1971); **27**, 700(E) (1971); **27**, 1550(E) (1971).
[32] Y. K. Gambhir and S. H. Patil, Z. Phys. A: At. Nucl. **321**, 161 (1985).
[33] Y. K. Gambhir and S. H. Patil, Z. Phys. A: At. Nucl. **324**, 9 (1986).
[34] M. Blann and H. K. Vonach, Phys. Rev. C **28**, 1475 (1983).
[35] C. Brusati, M. Cavinato, E. Fabrici, E. Gadioli, and E. Gadioli Erba, Z. Phys. A **353**, 57 (1995).
[36] A. De, T. Shibata, and H. Ejiri, Phys. Rev. C **45**, 774 (1992).
[37] G. A. Lalazissis, J. Konig, and P. Ring, Phys. Rev. C **55**, 540 (1997).
[38] A. Chatterjee, K. H. N. Murthy, and S. K. Gupta, Pramana **16**, 391 (1981).
[39] S. K. Charagi and S. K. Gupta, Phys. Rev. C **41**, 1610 (1990).
[40] A. Gavron, Phys. Rev. C **21**, 230 (1980).
[41] O. B. Tarasov and D. Bazin, Nucl. Instrum. Methods B **204**, 174 (2003).
[42] R. Bass, Nucl. Phys. A **231**, 45 (1974).
[43] C. M. Perey and F. G. Perey, Nucl. Data Tables **17**, 1 (1976).